Build Simul (2024) 17: 1693–1708
https://doi.org/10.1007/s12273-024-1167-9

Energy performance analysis of multi-chiller cooling systems for data centers concerning progressive loading throughout the lifecycle under typical climates

Yingbo Zhang[1], Hangxin Li[1] (✉), Shengwei Wang[1,2] (✉)

1. Department of Building Environment and Energy Engineering, The Hong Kong Polytechnic University, Hong Kong, China
2. Research Institute for Smart Energy, The Hong Kong Polytechnic University, Hong Kong, China

Abstract

The increasing demand for cooling energy in data centers has become a global concern. Existing studies lack a comprehensive analysis of the energy performance of widely used multi-chiller cooling systems in air-cooled data centers throughout their lifecycle, especially concerning progressive loading. To bridge this gap, this study conducts a thorough assessment of the energy performance of multi-chiller cooling systems throughout the entire lifecycle. Additionally, the impact of climate conditions on the energy efficiency of the cooling systems is analyzed, considering design variations for typical climates. Multi-chiller cooling system models are developed using the test data of cooling equipment and typical control algorithms. The energy performance of the cooling system is thoroughly analyzed under full-range cooling loads and climate conditions. Results show that free cooling time could differ up to 1442 hours at different part load ratios in the same location. Furthermore, the cooling system's coefficient of performance (COP) varies significantly, by up to 6, at different part load ratios, corresponding to a difference in power usage effectiveness (PUE) up to 0.14. Notably, the average cooling system COP throughout the lifecycle loading is found to be only 11.7, 2.9 lower than the design system COP.

Keywords

data center
cooling system
energy performance
life-cycle operation
power usage effectiveness (PUE)
coefficient of performance (COP)

Article History

Received: 25 April 2024
Revised: 10 July 2024
Accepted: 17 July 2024

© Author(s) 2024

1 Introduction

Energy-intensive data centers have become an increasing concern worldwide due to their high energy consumption. Global data center electricity use in 2021 was 220–320 TWh (Zhang et al. 2023), equivalent to 1%–1.5% of global electricity (Masanet et al. 2020; Liu et al. 2023). Cooling energy in data centers typically accounts for approximately 30%–40% of total energy consumption (Mitchell-Jackson et al. 2003). Data center cooling systems can be broadly classified into two main categories: (i) air-cooled data centers (Chen et al. 2023) including chilled-water cooling systems (air/water-cooled chillers) (Gupta et al. 2020), direct expansion cooling systems (Capozzoli and Primiceri 2015), direct/indirect air (evaporative) cooling systems (Liu et al. 2018); (ii) liquid-cooled data centers (Zhou et al. 2023), including direct/indirect liquid cooling (Habibi Khalaj and Halgamuge 2017). Among these cooling systems, chilled-water cooling systems equipped with water-side economizers are the most widely used in large data centers due to their high reliability (Niemann et al. 2011) and physical practicality (Taylor 2014).

Existing studies on the energy efficiency of chilled-water cooling systems have largely concentrated on the influence of climatic conditions. Lei and Masanet (2020) used Sobol's method to develop a model capable of predicting power usage effectiveness (PUE) across different cities. Their findings highlight that climate parameters are the most crucial factors in predicting PUE for water-side economizer systems. Díaz et al. (2020) conducted a study to explore the potential of water-side economizers under various climate conditions. They found that the coefficient of performance (COP) of the system could be increased by over 10% during wintertime in coastal climates. Cheung and Wang (2019) investigated the energy efficiency of the multi-chiller cooling system across different climate zones. They found

E-mail: Hangxin Li (hangxin.li@polyu.edu.hk); Shengwei Wang (beswwang@polyu.edu.hk)

List of symbols

N	number of cooling equipment
P	power consumption (kWh)
Q	cooling load (kW)
T	temperature (°C)
W	energy consumption (kWh)
CDP	cooling water pump
CHP	chilled water pump
COP	coefficient of performance
CRAH	computer room air handler unit
HVAC	heating, ventilation, and air conditioning
PLR	part load ratio
PUE	power usage effectiveness

Subscripts

ch	chiller
chw	chilled water
cooling	cooling system
ct	cooling tower
design	design condition
hx	heat exchanger
IT	IT equipment
op	operation
others	other losses
out	outlet
req	required
set	setpoint
wet	wet bulb

that cooling energy savings can be achieved by up to 15% in climate Zone 3B when adopting their optimal design.

On the other hand, some studies conducted energy performance assessments of cooling systems that incorporate technical enhancements or novel approaches (Ma et al. 2020). Mi et al. (2023) investigated the energy efficiency of the water-side free cooling system in data centers, specifically focusing on the optimization of cooling tower operation. Zou et al. (2023) studied the energy-saving potential of two retrofit strategies that integrate water-side economizers in data centers. They found that a loop thermosyphon system with a water-side economizer could reduce annual energy consumption by 53.4%–63.6%. Li and Li (2020) assessed the energy performance of data center cooling systems equipped with water-side economizers, focusing on the optimization of free cooling switchover temperature and cooling tower approach temperature. Their results show that significant energy savings, up to 10%, could be achieved by optimizing these parameters. Lyu et al. (2022) analyzed the benefits of deploying magnetic bearing chillers for data center cooling applications. They concluded that using magnetic bearing chillers could reduce cooling energy consumption by 10%–40% when compared to conventional centrifugal chillers.

Exiting studies have contributed valuable insights into the energy efficiency assessment of the chilled-water cooling system with water-side economizers, focusing on various climate conditions or technical optimizations. However, there remains a gap in the research regarding the energy performance of multi-chiller cooling systems in data centers throughout the lifecycle, particularly under conditions of progressive loading. A unique characteristic of data centers is that they typically operate at the progressive increase in IT load throughout their lifetime (Rasmussen 2011). It has been reported that most data centers operate at part load for the majority of their lifetime (Griffin 2015). Therefore, achieving high efficiency at these part loads is a key area of research for HVAC systems and cooling plants in data centers. In addition, the impact of variations in system designs for freeze protection on the energy efficiency of data center cooling systems in different climates has not been considered in existing research. Freeze protection is a crucial consideration, particularly in colder climates. Different system designs for freeze protection could affect the overall energy efficiency of cooling systems.

This study presents a pioneering and comprehensive energy performance assessment of widely used multiple water-cooled chillers for air-cooled data centers concerning progressive loading throughout the lifecycle. Multi-chiller cooling system models are developed using the test data of cooling equipment and typical control algorithms. The models take into account the variations in system designs related to freeze protection across different climatic conditions. The energy performance of cooling system components is thoroughly analyzed under full-range cooling loads and climate conditions. Additionally, free cooling hours, cooling system COP (coefficient of performance), and data center PUE (power usage effectiveness) under full-range cooling loads are identified and analyzed. More importantly, the energy performance of the cooling system is quantified under a typical progressive loading experienced over the data center's lifecycle. The quantitative results are valuable for designing optimal cooling systems and achieving high-efficiency cooling systems at partial loads throughout the data center's lifecycle. This study provides significant insights into the energy efficiency and performance of multi-chiller cooling systems for air-cooled data centers throughout the lifecycle and guides the development of

next-generation high-efficiency cooling systems for data centers.

2 Methodology

This section introduces the specification of multi-chiller cooling systems in the referenced data center, the modeling of the cooling system, and typical operation modes as well as control algorithms. The outline of the assessment procedure is elaborated as shown in Figure 1.

i. The cooling system models are developed using the test data of cooling equipment and typical control algorithms using the software TRNSYS 18. The models consider the variations in system designs related to freeze protection for different climates.
ii. Python programming is used to change inputs, such as weather data and cooling loads, within the cooling system model created in TRNSYS 18. Additionally, Python programming is used to determine the optimal operation mode for each specific weather condition and cooling load.

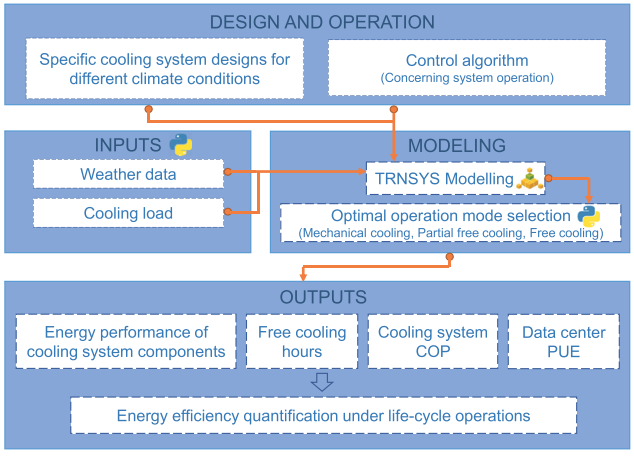


Fig. 1 Procedure and steps of energy performance assessment

iii. The energy performance of the cooling system components, as well as relevant metrics such as free cooling hours, cooling system COP, and data center PUE, are identified under full-range cooling loads and climate conditions.
iv. The energy performance of the cooling system is quantified throughout the lifecycle with a typical progressive loading scenario.

2.1 Multi-chiller cooling systems of the referenced data center

2.1.1 Specifications of the referenced data center

The cooling system design of the reference date center is shown in Figure 2 (Cheung and Wang 2019). The design considered distribution headers around all cooling towers and all cooling water pumps, and the combination of constant-speed cooling water pumps with different flow capacities. Distribution headers around all cooling towers allow the use of more cooling towers than chillers and water-side economizers, which increases heat rejection area in the cooling process and subsequently enhances cooling efficiency. Distribution headers around all cooling water pumps can reduce the number of operating pumps under part load conditions, and then increase the energy efficiency of all pumps. The combination of constant-speed cooling water pumps with different flow capacities could make cooling water pumps work efficiently under part load conditions.

The total cooling load of the data center is 16800 kW (Cheung and Wang 2019). The data center cooling system is equipped with four water-cooled chillers, four water-side economizers, four variable cooling towers, two large constant-speed cooling water pumps (CDP), two small constant-speed cooling water pumps, and four chilled water pumps (CHP). Detailed specifications for each piece of cooling

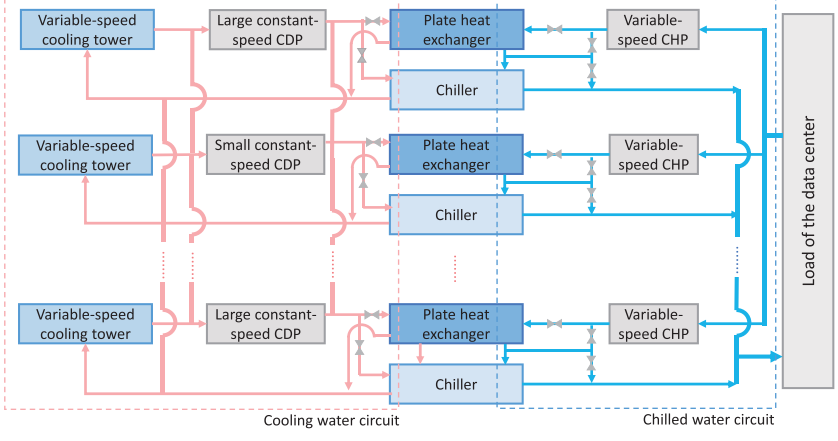


Fig. 2 Schematic of the multi-chiller cooling system

equipment are provided in Table 1. For a fair comparison, both the selected open cooling tower and the closed-circuit cooling tower are equipped with axial fans and largely the same design heat rejection capacity from the same manufacturer.

2.1.2 Typical operation modes

There are three typical operation modes for water-cooled multi-chiller cooling systems in data centers, mechanical cooling mode, partial free cooling mode and free cooling mode, respectively.

Mechanical cooling mode: There are two circuits in cooling systems. One is the cooling water circuit, and the other is the chilled water circuit. In the cooling water circuit, the heated cooling water from a chiller flows to a cooling tower and then is cooled through the heat dissipation of a cooling tower. The cooled cooling water enters a chiller. In the chilled water circuit, the chilled water from a chiller enters the computer room air handler and then cools hot air in the computer room. The heated chilled water goes back to the chiller. The mechanical cooling mode does not involve the plate heat exchanger.

Table 1 Specification of the data center cooling system in the case study

Equipment	Design specification	Quantity
Water-cooled chiller	Design cooling capacity: 4200 kW Design chilled water outlet temperature: 13 °C Design chilled water flow rate: 544300 kg/h Design cooling water flow rate: 620000 kg/h	4
Water-side economizer	Design heat transfer rate: 4300 kW Design water flow rate: 620000 kg/h	4
Variable-speed chilled water pump	Design flow rate: 620000 kg/h Design pressure head: 500 kPa Design power consumption: 110 kW	4
Large constant-speed cooling water pump	Design flow rate: 1240000 kg/h Design pressure head: 350 kPa Design power consumption: 145 kW	2
Small constant-speed cooling water pump	Design flow rate: 620000 kg/h Design pressure head: 350 kPa Design power consumption: 84 kW	2
Variable-speed open cooling tower	Design power consumption: 74 kW Design airflow rate: 235.6 m^3/s Design heat rejection rate: 16800 kW Design power for anti-freezing electric heater: 60 kW	4
Variable-speed closed-circuit cooling tower	Design power consumption: 110 kW Design heat rejection rate: 16800 kW Design airflow rate: 268.88 m^3/s Design water flow rate: 1071429 kg/h	4

Partial free cooling mode: The cooling water from a cooling tower enters a heat exchanger. Meanwhile, the heated chilled water by hot air in a computer room also enters a heat exchanger. The heat exchanger precools the heated chilled water. The pre-cooled chilled water enters a chiller and then is further cooled by the chiller to achieve the desired chilled water supply temperature. The chilled water further cooled by the chiller enters a computer room to exchange heat with the hot air. Meanwhile, the heated cooling water from the heat exchanger and the chiller both returns to the cooling tower. This mode involves chillers and heat exchangers. Heat exchangers are used to precool and handle part of the cooling load.

Free cooling mode: In the cooling water circuit, the cooling water from a cooling tower enters the heat exchanger, and then exchanges heat with heated chilled water from a computer room. After heat exchange, the heated cooling water returns to a cooling tower for the cooling water circuit. For the chilled water circuit, the chilled water from a heat exchanger enters the computer room air handler and then exchanges heat with hot air in the computer room. The free cooling mode does not involve a chiller, and heat exchangers handle all cooling loads.

2.1.3 Typical control algorithms of the cooling system

This section elaborates on control algorithms used in the case study. The control algorithms involve the operation mode of the cooling system and the operation of the cooling equipment.

The operation mode of the cooling system: Figure 3 shows the procedure for selecting the optimal operation mode. First, all three cooling modes will be simulated under each cooling load and ambient air temperature. Then, according to the simulation results, the cooling modes that can meet the cooling load could be identified. Last, the one exhibiting the lowest power consumption will be selected as the optimal operation mode.

Number of chillers, heat exchangers and cooling towers in operation: The number of operating chillers and economizers varies from the operation mode. The principle of operating equipment quantity is to meet the cooling load. The number of cooling towers is larger than the number of operating chillers and waterside economizers to increase the heat rejection area. To avoid a lack of water in operating cooling towers, the number of cooling towers in operation is one more than the number of chillers and economizers in operation. Table 2 shows the number of chillers, heat exchangers, and cooling towers in operation in three cooling modes.

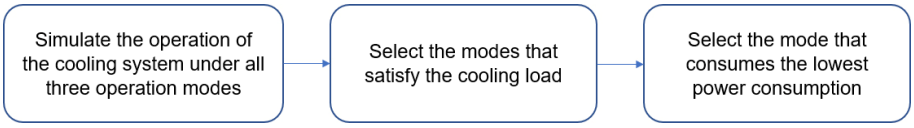


Fig. 3 Procedure to select the optimal operation mode

Table 2 Number of chillers, water-side economizers, and cooling towers in operation

Operation mode	Cooling load (kW)	Number of chillers in operation	Number of water-side economizers in operation	Number of cooling towers in operation
Mechanical cooling	< 4200 kW	1	0	2
	4200–8400 kW	2	0	3
	8400–12600 kW	3	0	4
	> 12600 kW	4	0	4
Partial free cooling	< 8500 kW	1	1	2
	> 8500 kW	2	2	3
Free cooling	< 4300 kW	0	1	2
	4300–8600 kW	0	2	3
	8600–12900 kW	0	3	4
	> 12900 kW	0	4	4

Chilled water supply temperature of chillers or heat exchangers: The chilled water supply temperature is set at 13 °C. It is common to set the chilled water supply temperature at 13 °C (then the supplying cold air is 20–22 °C) or even higher, in line with the recommended space temperature (20–27 °C) in data centers, according to ASHRAE standard (ASHRAE 2021). In mechanical cooling and partial free cooling mode, the chilled water supply temperature is achieved by chillers. In free cooling mode, the chilled water supply temperature is achieved by controlling the fan speed of the cooling towers.

Number of pumps in operation: In the study, the number of chilled water pumps is the same as the maximum between the number of operating chillers and the number of operating economizers. The number of cooling water pumps is shown in Table 3.

Operating speed of variable speed water pumps: The number of operating chilled water pumps is the maximum between the number of operating chillers and the number of operating heat exchangers. The speed of chilled water pumps is controlled according to the required total chilled water flow rate (Equation (1)). The speed limits of the chilled water pumps are 30 Hz to 50 Hz to protect their motors. Therefore, the frequency of chilled water pumps when the number of chillers or heat exchangers changes.

Table 3 Number of operating cooling water pumps in operation

Total required cooling water flow	Number of operating cooling water pumps
< 620000 kg/h	1 small pump
620000–1240000 kg/h	1 large pump
1240000–1860000 kg/h	1 large pump and 1 small pump
> 1860000 kg/h	2 large pumps

The speed of large and small constant-speed cooling water pumps always remains at 50 Hz.

$$\dot{m}_{\mathrm{req,chw}} = N_{\mathrm{op,ch}}\dot{m}_{\mathrm{des,chw,ch}} + N_{\mathrm{op,hx}}\dot{m}_{\mathrm{des,chw,hx}} \quad (1)$$

where, $\dot{m}_{\mathrm{req,chw}}$ is the required total chilled water flow rate, $N_{\mathrm{op,ch}}$ is the number of operating chillers, $N_{\mathrm{op,hx}}$ is the number of operating heat exchangers, $\dot{m}_{\mathrm{des,chw,ch}}$ is the design chilled water flow rate of the chiller (544300 kg/h), $\dot{m}_{\mathrm{des,chw,hx}}$ is the design chilled water flow rate of the heat exchanger (620000 kg/h).

Operating speed of cooling tower fans: The speed of the variable-speed fans in cooling towers depends on the operation mode and the ambient wet-bulb temperature. In free cooling mode, the speed of cooling tower fans is controlled according to the principle that the water supply temperature of water-side economizers reaches 13 °C. In mechanical cooling and partial free cooling mode, the supplied chilled water is controlled by chillers. The speed of the fans is controlled to maintain the cooling tower water outlet temperature at the set point, given by Equation (2). The setpoint ensures optimal performance of the fan and considers the chiller minimum condenser water entering temperature (Wang 2009). In addition, the spray-water pump of the closed-circuit cooling tower is shut off for freeze protection if the outdoor temperature is lower than 0 °C.

$$T_{\mathrm{ct,out,set}} = \mathrm{Max}(T_{\mathrm{wet}} + 5[^{\circ}\mathrm{C}], 18[^{\circ}\mathrm{C}]) \quad (2)$$

The temperature difference between air supply and return in computer rooms: the temperature difference between air supply and return in computer rooms is fixed at 10 °C (ASHRAE 2009; Gözcü et al. 2017). In addition, since the environment of computer rooms is isolated, there is no humidification requirement in the cooling system (Gözcü and Erden 2019).

2.2 Modelling of the cooling system concerned

The operation of the data center cooling system is simulated using TRNSYS 18, with the majority of cooling equipment having been well validated by previous studies according to the TRNSYS 18 user manual (http://sel.me.wisc.edu/trnsys). In addition, typical meteorological year (TMY) weather files (https://energyplus.net/) were used in the simulations.

Chillers are modeled using Type 142, which relies on catalog data provided as external text files to determine chiller performance. The performance testing data of the chiller used in this study is from a major manufacturer (York). Tables 4 and 5 summarize and present the PLR and performance input data of Type 142 used in this study.

Open cooling towers are modeled using Type 162. Closed-circuit cooling towers are modeled using Type 510. The design parameters of cooling tower models are presented in Table 1. The ε-NTU method is used to model open cooling tower. Air effectiveness (ε_a) can be determined using the relationships for sensible heat exchangers with modified definitions for the number of transfer units and the capacitance rate ratios, using the assumption that the Lewis number equals one (Braun 1988). For a counterflow cooling tower, it is described as Equation (3).

$$\varepsilon_a = \frac{1-\exp\left(-\mathrm{NTU}\left(1-m^*\right)\right)}{1-m^*\exp\left(-\mathrm{NTU}\left(1-m^*\right)\right)} \tag{3}$$

$$\mathrm{NTU} = \frac{h_D A_v V_{cell}}{m_a} \tag{4}$$

Table 4 The PLR data of chiller model Type 142

PLR	Fraction of full power
0.15	0.165
0.2	0.195
0.3	0.262
0.4	0.328
0.5	0.398
0.6	0.480
0.7	0.580
0.8	0.698
0.9	0.843
1	1

Table 5 The performance data of chiller model Type 142

Chilled water supply temperature	Cooling water supply temperature	Chiller COP
7	18	7.021
7	22	6.310
7	24	6.207
7	28	5.979
7	32	5.478
10	18	8.020
10	22	7.182
10	24	6.407
10	28	6.154
10	32	5.807
12	18	9.729
12	22	8.554
12	24	7.964
12	28	7.071
12	32	6.208
15	18	11.438
15	22	9.908
15	24	9.298
15	28	8.073
15	32	7.034

$$m^* = \frac{m_a C_s}{m_{w,i} C_{pw}} \tag{5}$$

where, h_D is the mass transfer coefficient, A_v is the surface area of water droplets per tower cell exchange volume, V_{cell} is the total tower cell exchange volume, m_a is the mass flow rate of air, $m_{w,i}$ is the mass flow rate of the inlet water, C_{pw} is the constant pressure specific heat of water, and C_s is the saturation-specific heat.

The wet-bulb temperature is used as a primary input of the open cooling tower model because the enthalpy can be approximated as a formula related to wet-bulb temperature (Ma et al. 2008), at a given atmospheric pressure. According to the desired cooling capacity for cooling towers and outdoor conditions, the airflow rate can be determined. The fan power is in cubic growth of the rotational speed as shown in Equation (6) (Lu et al. 2015).

$$\frac{P_{ct}}{P_{ct,design}} = \left(\frac{Q_{ct}}{Q_{ct,design}}\right)^k \tag{6}$$

where, P_{ct} is the energy consumption of cooling towers. $P_{ct,design}$ is the energy consumption of cooling towers at the design condition. Q_{ct} is the airflow rate, and $Q_{ct,design}$ is the airflow rate at the design condition.

Closed cooling towers rely on the basic premise that the saturated air temperature is the temperature at the air–water

interface and is also the temperature of the outlet fluid. The saturated air enthalpy can be calculated by Equation (7).

$$h_{sat}\left(T_{fluid,out}\right) = h_{air}\left(T_{air,in}\right) + \frac{\dot{Q}_{fluid}}{\dot{m}_{air}\left(1-\exp\left[-\beta_{design}\left(\frac{\dot{m}_{air}}{\dot{m}_{air,design}}\right)^{y-1}\right]\right)} \quad (7)$$

$$\beta_{design} = \ln\left[\frac{h_{sat}\left(T_{fluid,out,design}\right)-h_{air}\left(T_{air,in,design}\right)}{h_{sat}\left(T_{fluid,out,design}\right)-h_{air}\left(T_{air,out,design}\right)}\right] \quad (8)$$

where, $h(T)$ is the enthalpy at the given temperature T, $\dot{m}$ is the mass flow rate, $\dot{Q}$ is the heat transfer rate, and y = 0.6 for most applications.

The outlet air enthalpy could be found from an energy balance on the cooling tower and can be expressed as:

$$\dot{Q}_{fluid,design} = \dot{m}_{fluid} C_{p,fluid}\left(T_{fluid,in,design} - T_{fluid,out,design}\right) \quad (9)$$

$$h_{air}\left(T_{air,out,design}\right) = h_{air}\left(T_{air,in,design}\right) + \frac{\dot{Q}_{fluid,design}}{\dot{m}_{air}} \quad (10)$$

The airflow rate is calculated by Equation (11). The fan power is in cubic growth of the airflow rate.

$$\dot{m}_{air} = \dot{m}_{air,design}\gamma_{air} \quad (11)$$

$$\gamma_{air} = \frac{\dot{m}_{air}}{\dot{m}_{air,design}} \quad (12)$$

where, γ is the ratio of flow rate to design flow rate.

The pump models are modified based on Type 743. The pump flow rate is calculated according to the speed of the pump and the pressure difference of the pipelines. The pressure difference of the pipeline is estimated by Equation (13), which is a variation from the widely used fan affinity law. Equation (14) shows the relationship between pump speed, pump pressure difference and pump flow rate (Cheung and Wang 2019).

$$\Delta P_{pipe} = \Delta P_{des,pump}\left(\frac{\dot{m}_{pump}}{\dot{m}_{des,pump}}\right)^2 \quad (13)$$

$$\Delta P_{pump} = c_{pump,0} f_{pump}^2 + c_{pump,1} f_{pump} \dot{m}_{pump}^2 \quad (14)$$

where, ΔP is the pressure difference, $\dot{m}_{pump}$ is the flow rate of operating pumps in its water circuit. $c_{pump,0}$ and $c_{pump,1}$ are the parameters of the pump model, f_{pump} is the speed of the pump. According to manufacturers' specifications of pumps, $c_{pump,0}$ is 0.023, and $c_{pump,1}$ is −3.9E−13 for chilled water pumps; $c_{pump,0}$ is 0.0178, and $c_{pump,1}$ is −1.89E−13 for small cooling water pumps; $c_{pump,0}$ is 0.0177, and $c_{pump,1}$ is −1.32E−13 for large cooling water pumps.

Heat exchangers are modeled using Type 657. In the heat exchanger model, the energy transfer across the heat exchanger is given by Equation (15)

$$Q_{hx} = \varepsilon C_{min}\left(T_{hot,in} - T_{cold,in}\right) \quad (15)$$

where, Q_{hx} is the energy transfer across the heat exchanger, ε is the heat exchanger's effectiveness, 0.857 in this study according to manufacturing testing data, C_{min} is the minimum of the hot and cold-side fluid thermal capacitances, $T_{hot,in}$ is the temperature of fluid entering the hot side of the heat exchanger.

CRAH is modeled according to the Equation (16). A variable-speed fan that changes airflow based on the cooling load was applied to the CRAH in the reference data center (Ham et al. 2015b). The difference between supply and return air temperatures of the computer rooms is assumed to be a constant of 10 K (ASHRAE 2009).

$$\frac{P_{CRAH}}{P_{CRAH,des}} = \frac{\dot{V}_{SA}^3}{\dot{V}_{SA,des}^3} \quad (16)$$

where, P_{CRAH} is the power consumption of CRAH, $\dot{V}_{SA}$ is the airflow rate.

2.3 Cooling system designs and performance metrics

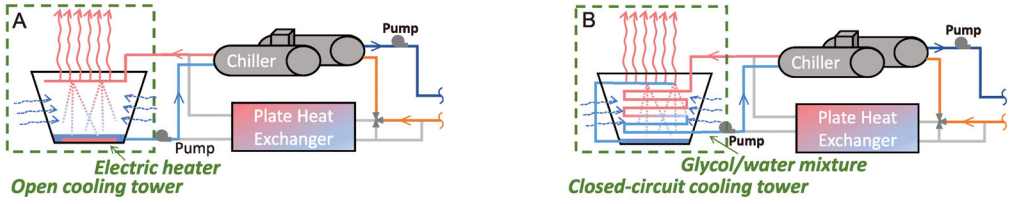
2.3.1 *Cooling system designs for different climate conditions*

In practice, the implementation of identical cooling systems in data centers situated in different climatic conditions often necessitates modification in design and operation to address the specific needs and constraints associated with each climate. Table 6 shows six cities located in different climate conditions and their specific designs.

Figure 4 shows specific designs for freeze protection in water-cooled cooling systems. Generally, open cooling towers are widely used in the cooling system due to their high heat rejection efficiency and low capital cost (Stabat and Marchio 2004; Taylor 2012), shown in Figure 4A. To prevent freezing, electric heaters are installed inside open cooling towers for freeze protection and are activated under necessary or extreme conditions. However, in regions experiencing exceptionally harsh winter, where outdoor air temperature can reach −35 °C, such as Harbin. Electric heaters may prove inadequate for preventing freeze-related issues according to engineering cases. For such extreme cold environments, closed-circuit cooling towers and antifreeze solutions are adopted for freeze protection (ASHRAE 2020), as shown in Figure 4B. The antifreeze solution used in the closed-circuit cooling tower typically consists of a mixture of water and ethylene glycol.

Table 6 Selected climate zones and cities

Zone	City	Longitude and latitude	Specific design
Hot summer and warm winter	Hong Kong	22.3°N and 114.2°E	Figure 4A
Temperate	Kunming	25.0°N and 102.7°E	Figure 4A
Hot summer and cold winter	Shanghai	31.2°N and 121.4°E	Figure 4A
Cold	Beijing	39.9°N and 116.3°E	Figure 4A
Severe cold	Ulanqab	40.1°N and 110.3°E	Figure 4A
Extremely severe cold	Harbin	45.8°N and 126.8°E	Figure 4B



Design for most regions

Specific design for extremely cold regions

Fig. 4 Schematic of specific cooling system designs

2.3.2 *Data center energy flow and performance metrics*

Electricity energy flow in data centers

Figure 5 shows the electrical energy flow in a data center (Iyengar et al. 2010; Joshi and Kumar 2012). In a typical data center, electrical energy is supplied from the utility grid to power uninterruptible power supply (UPS) systems, cooling systems as well as other miscellaneous equipment (e.g., lighting and offices). UPS provides power to the IT equipment. Generally, there will be electricity losses at UPS. In this study, UPS electricity loss and other miscellaneous electricity consumption are considered to account for 12% of the IT electricity consumption (Gözcü et al. 2017; Lei and Masanet 2020).

Power usage effectiveness (PUE)

In the data center industry, the most used metric that evaluates the energy effectiveness of the data center is Power Usage Effectiveness (PUE). PUE was proposed in 2006 (Malone and Belady 2006) and promoted by the Green Grid (a non-profit organization of IT professionals) in 2007 (Green Grid 2007). PUE is an indicator of the energy efficiency of data centers. A lower PUE represents a more efficient data center. It means that more electrical energy is used by IT equipment instead of other equipment. A PUE of 1 is an ideal value (Brady et al. 2013).

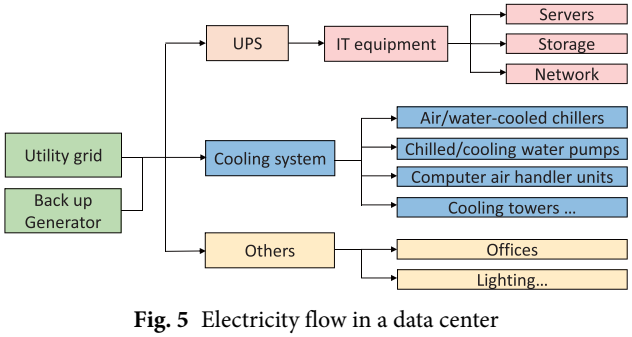


Fig. 5 Electricity flow in a data center

$$\text{PUE} = \frac{\text{Total facility power}}{\text{IT equipment power}} = \frac{P_{\text{IT}} + P_{\text{cooling}} + P_{\text{others}}}{P_{\text{IT}}} \quad (17)$$

Energy efficiency of cooling systems

To further analyze the energy performance and efficiency of data center cooling systems, the coefficient of cooling system performance (COP) is proposed, given by Equation (18) (Cheung and Wang 2019).

$$\text{Cooling system} \qquad \text{COP} = \frac{Q}{W_{\text{system}}} \quad (18)$$

where Q is the cooling load and W_{system} is the energy consumption of the data center cooling system, including the energy consumption of the cooling plant and the computer room air handler (CRAH).

In addition, the part load ratio (PLR) is defined by Equation (19). The cooling load in data centers is dominated by the servers themselves. Therefore, the impact of weather-related cooling load variations in different cities is often considered negligible in studies related to data center cooling systems (Cho et al. 2015; Ham et al. 2015a; Díaz et al. 2020).

$$\text{PLR} = \frac{\text{Actual cooling load}}{\text{Design cooling load}} \quad (19)$$

3 Energy performance under full-range loads and climate conditions

3.1 Energy performance of cooling system components

The cooling system is designed with a total of four cooling equipment units. According to the control algorithms of the cooling system, the part load ratios (PLRs) of 0.25, 0.5, and 0.75 are transition points where the number of chillers would increase or decrease.

Figure 6 (corresponding to the specific design shown in Figure 4A) and Figure 7 (corresponding to the specific design shown in Figure 4B) illustrate the energy performance of cooling system components under full-range loads and

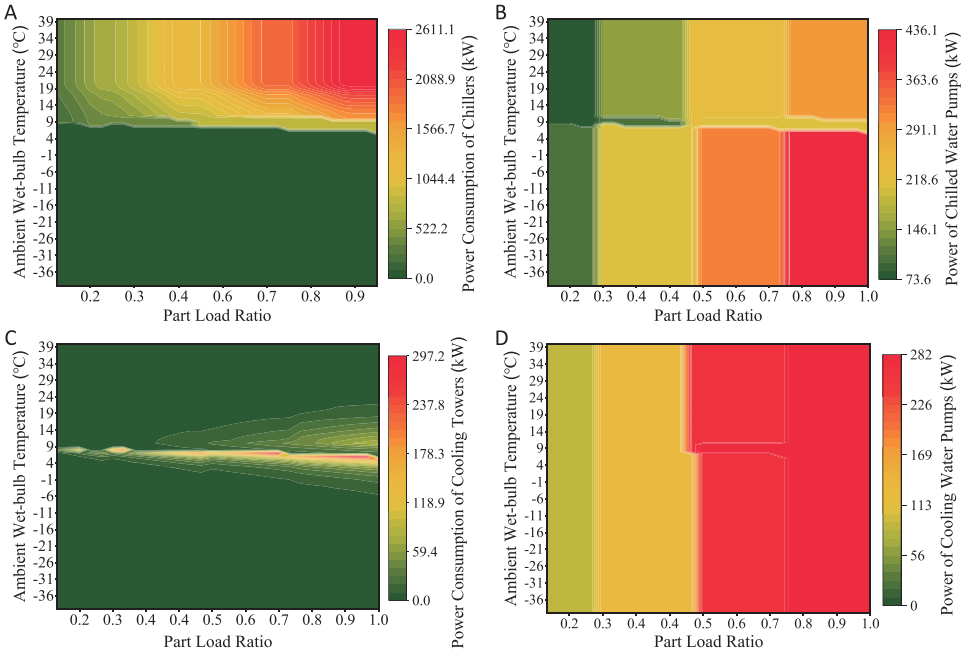


Fig. 6 Energy performance of cooling system components with the specific design (Figure 4A), chiller (A), chilled water pump (B), open cooling tower (C), and cooling water pump (D)

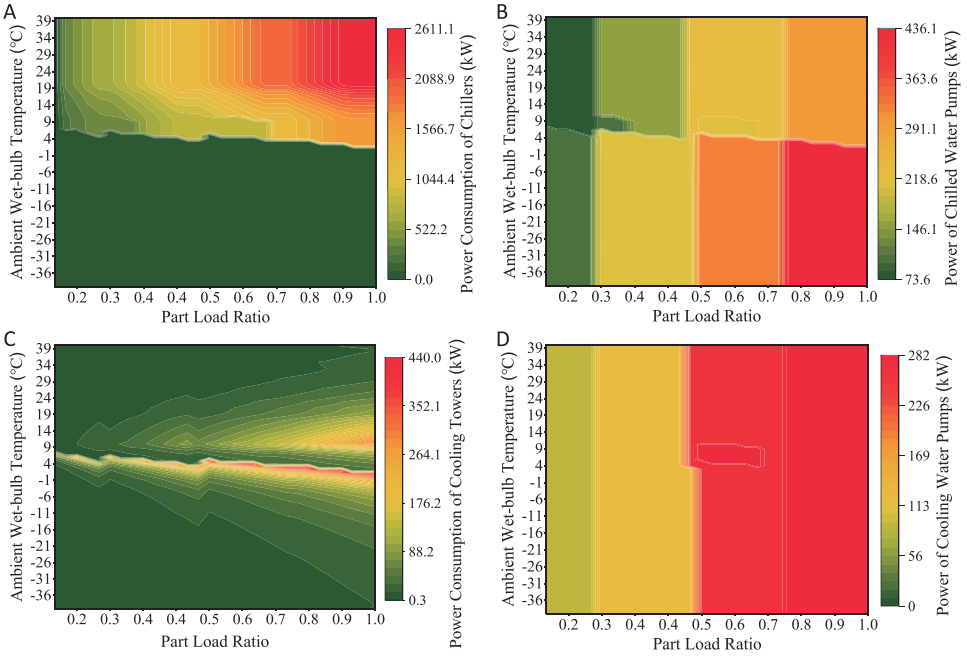


Fig. 7 Energy performance of cooling system components with the specific design (Figure 4B), chiller (A), chilled water pump (B), closed-circuit cooling tower (C) and cooling water pump (D)

ambient wet-bulb temperatures. Notably, there are distinct dividing lines that fluctuate within the range of 3–9°C for four components. These wet-bulb temperatures serve as crucial switching points for different operation modes of the cooling system, such as the transition from mechanical cooling to partial free cooling or from partial free cooling to free cooling.

In Figure 6(A) and Figure 7(A), the power consumption of chillers rises as wet-bulb temperature increases (chillers are in operation when wet bulb temperature exceeds 9 °C). This is due to the fact that there is a lower chiller COP when the cooling water temperature is higher. As the ambient air temperature increases, the cooling water outlet temperature from the cooling tower also increases according to the control algorithm of cooling towers (Equation (2)). Additionally, it is observed that the power consumption of chillers increases as cooling system PLR increases, and increases slowly when PLR is near 0.2 (one chiller in operation), 0.4 (two chillers in operation), 0.6 (three chillers in operation) and 0.8 (four chillers in operation). This can be attributed to the fact that each chiller operates at a chiller PLR of 0.8 when the cooling system PLR is near 0.2, 0.4, 0.6 and 0.8. The chiller COP increases as the chiller PLR rises, reaches its peak at a chiller PLR of approximately 0.8, and then experiences a slight decrease as the PLR continues to increase to 1.

In Figure 6(B, D) and Figure 7(B, D), there are sudden increases in the power consumption of chilled water pumps and cooling water pumps when the PLR approaches 0.25, 0.5 and 0.75. The reason is that the change in cooling load directly impacts the number of chilled water pumps in operation. Notably, the power consumption of chilled water pumps varies across different operation modes in Figure 6(B) and Figure 7(B). This variation can be attributed to the specific control algorithm of chilled water pumps, as described by Equation (1). The change in power consumption of cooling water pumps (in Figure 6(D) and Figure 7(D)) is due to the adjustment in the number of cooling water pumps in operation.

The main difference between the two specific designs lies in the energy performance of cooling towers. In general, closed cooling towers, as shown in Figure 7(C), consume more power compared to open cooling towers shown in Figure 6(C). Notably, there is a noticeable dividing line at wet-bulb temperatures ranging from 5 °C to 9 °C for open cooling towers (Figure 6(C)), and from 3 °C to 7 °C for closed-circuit cooling towers (Figure 7(C)). The wet-bulb temperature in the dividing line is the switching temperature for different operation modes at different PLRs.

The switch temperatures for operation modes adopting closed-circuit cooling towers are lower than those adopting open cooling towers. This difference can be attributed to the lower cooling efficiency of closed-circuit cooling towers, as they do not have direct contact between the cooling water and the outdoor cold air (Taylor 2012). In addition, the use of antifreeze solutions in closed-circuit cooling towers results in lower specific heat capacity and a consequently lower convective heat transfer coefficient in heat exchangers, and therefore a larger approach temperature for heat exchangers.

3.2 Overall energy performance of data centers

3.2.1 Free cooling hour under full-range cooling loads

Figure 8 illustrates the operating hours of three cooling modes (free cooling, partial free cooling and mechanical cooling) at different part load ratios (PLR) throughout the year in six representative cities. Among these cities, Ulanqab shows the maximum free cooling hours, reaching 5921 hours at a PLR of 1. Following Ulanqab, the cities of Harbin, Kunming, Shanghai, Beijing, and Hong Kong show decreasing free cooling hours. Hong Kong shows the minimum free cooling hours, only 158 hours. Furthermore, it can be observed that the number of free cooling hours decreases as the PLR increases in all cities. For example, in Kunming, the free cooling hours decrease by up to 1442 hours throughout the year when the PLR increases from 0.1 to 1. The variation in free cooling hours in different cities is mainly due to the change in the switching point from partial free cooling mode to free cooling mode. For example, when the partial load ratio (PLR) is 0.3, the switching wet-bulb temperature from partial free cooling mode to free cooling mode is 11 °C. When the PLR is 1, the switching wet-bulb temperature from partial free cooling mode to free cooling mode is 8 °C. This means that the free cooling hours will decrease by the total hours at the wet-bulb temperatures of 9–11 °C in different cities. The total hours at wet-bulb temperatures of 11 °C, 10 °C, and 9 °C vary in different cities, resulting in varying decreases in free cooling hours when the PLR increases. The change in switching wet-bulb temperature can be attributed to the fact that the cooling tower capacity is "oversized" when the cooling load is lower than the designed cooling load. Essentially, the "oversized" cooling towers have the capability to handle the cooling load even at higher wet-bulb temperatures than the design condition.

It is worth noting that there are rebounds in free cooling hours when the PLRs are 0.25 and 0.5. This is due to the change in the number of cooling towers in operation. According to control algorithms, the number of cooling towers in operation increases from 2 to 3 when the PLR is 0.25, and from 3 to 4 when the PLR is 0.5. When more cooling towers are activated, the total heat rejection area

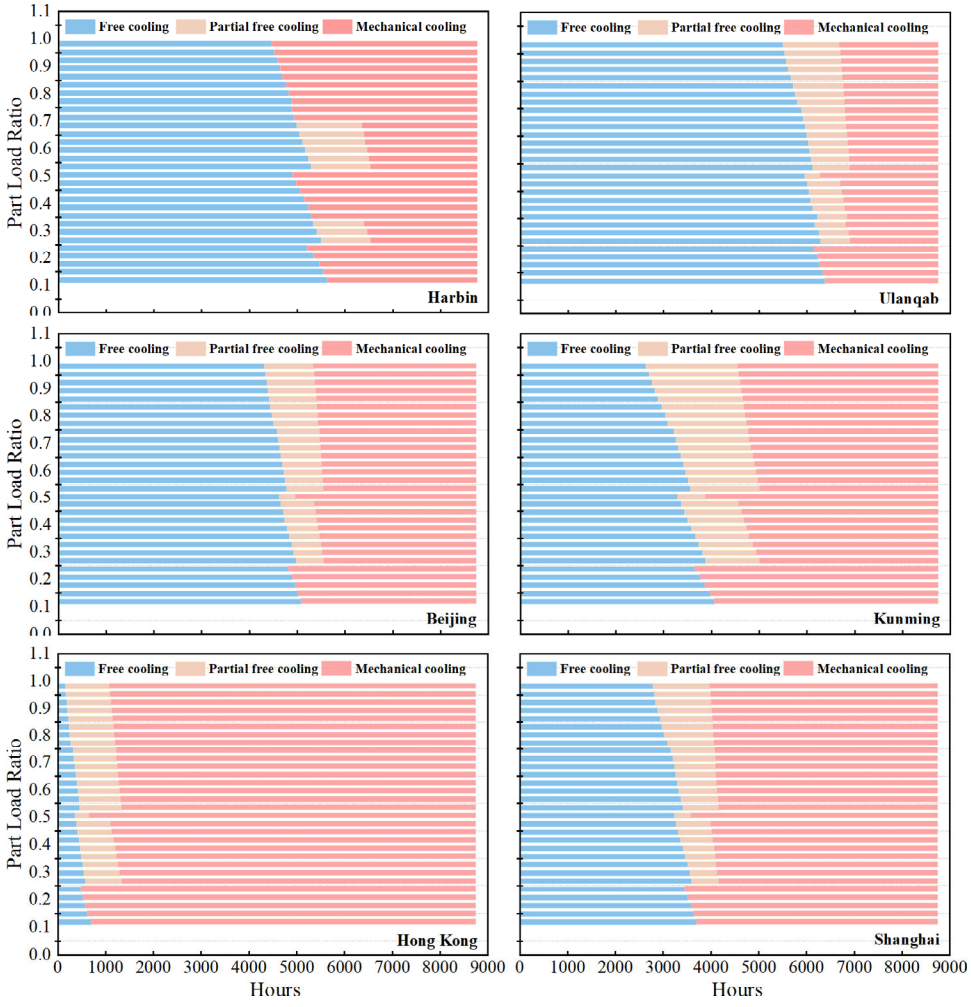


Fig. 8 Operating hours of three cooling modes in different cities

of the cooling towers also increases. This means that there is an "oversized" cooling tower capacity at PLRs of 0.25 and 0.5. The cooling towers have the capability to handle the cooling load even at higher wet-bulb temperatures. Consequently, there are more available free cooling hours that can meet the cooling load once the number of cooling towers increases at these critical switching points. Meanwhile, there is no rebound in free cooling hours at a PLR of 0.75. This is because the design quantity of cooling towers is 4 in this study. There is no increase in the number of cooling towers at a PLR of 0.75.

3.2.2 Energy performance under full-range cooling loads

Figure 9 shows the annual average data center PUE and cooling system COP at different part load ratios (PLRs) in six representative cities. The difference in cooling system COP at different PLRs can be as high as 6. Generally, cooling system COP increases as the part load ratio increases except for three significant drops in cooling system COP at the PLRs of 0.25, 0.5, and 0.75. As explained in Section 3.1, these PLRs act as transition points where the number of chillers in operation may increase or decrease. At these critical transition points, activating an additional chiller will result in multiple chillers operating at their off-design conditions and thus a decrease in cooling efficiency. For instance, when the part load ratio is close to and below 0.25, only one chiller is in operation, which operates at its design conditions and thus has a high chiller COP. However, when the PLR slightly exceeds 0.25, a second chiller is activated, causing both chillers to operate at their off-design conditions and resulting in a low chiller COP. As the PLR increases towards 0.5, both chillers can operate closer to their design conditions and thus a high chiller COP once again.

As the PLR increases, the data center PUE shows the opposite trend compared to the cooling system COP. This is due to the fact that a higher cooling system COP means low cooling energy consumption, resulting in a low PUE. The difference in data center PUE at different PLRs can be up to 0.14.

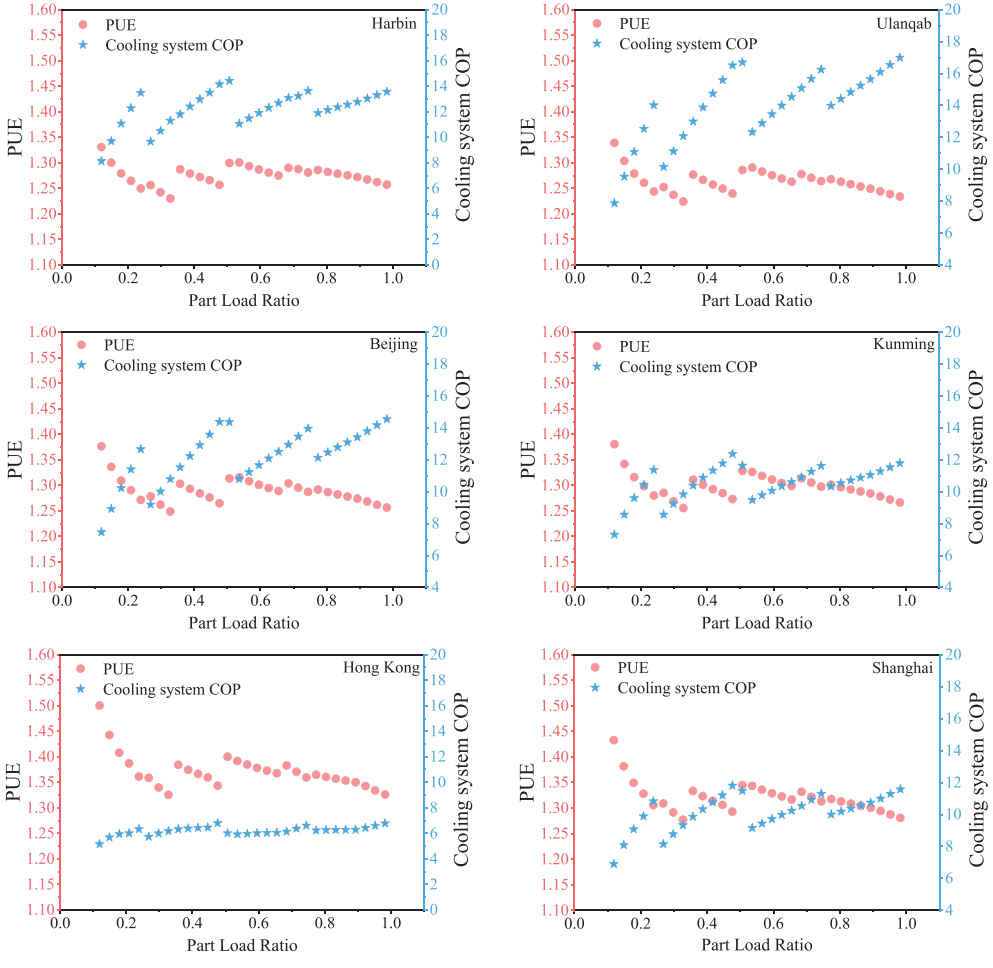


Fig. 9 Annual average data center PUE and cooling system COP at part load ratios in different cities

Figure 10 compares cooling system COP at PLRs of 0.9 and 1.0 over the typical year, taking Kunming as an example. There is no change in the number of cooling equipment at the PLRs of 0.9 and 1.0. It is observed that the cooling system COP at a PLR of 1.0 is consistently higher than that at a PLR of 0.9 even though the latter has higher free cooling hours. Several factors contribute to this observation. In free-cooling mode, the increased cooling loads necessitate a corresponding increase in energy consumption by the cooling towers. However, the increased energy consumption of the cooling towers is lower than the increased cooling loads. In mechanical-cooling mode and partial-free-cooling mode, the chillers play a key role in determining the total energy consumption. Similarly, the increased energy consumption of chillers is also lower than the increased cooling loads. Therefore, the cooling system operates more efficiently at a PLR of 1.0 compared to a PLR of 0.9.

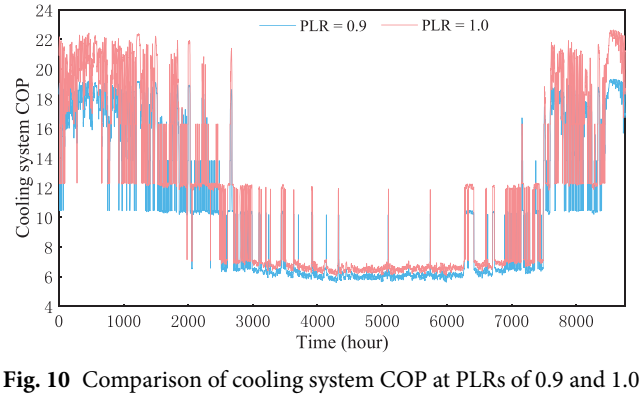


Fig. 10 Comparison of cooling system COP at PLRs of 0.9 and 1.0 over the typical year in Kunming

3.2.3 *Impact of climate condition on energy performance*

Figure 11(A) compares cooling system COP in six cities at different PLRs. The rankings of cooling system COP in these cities, from highest to lowest, are Ulanqab, Harbin, Beijing, Kunming, Shanghai, and Hong Kong. The primary reason for the difference in cooling system COP among these cities is the distribution of annual wet-bulb temperatures. The determinant is the number of hours below the critical wet-bulb temperature, which triggers the data center cooling system to switch from free-cooling mode to other modes. This indicates that Ulanqab experiences more favorable

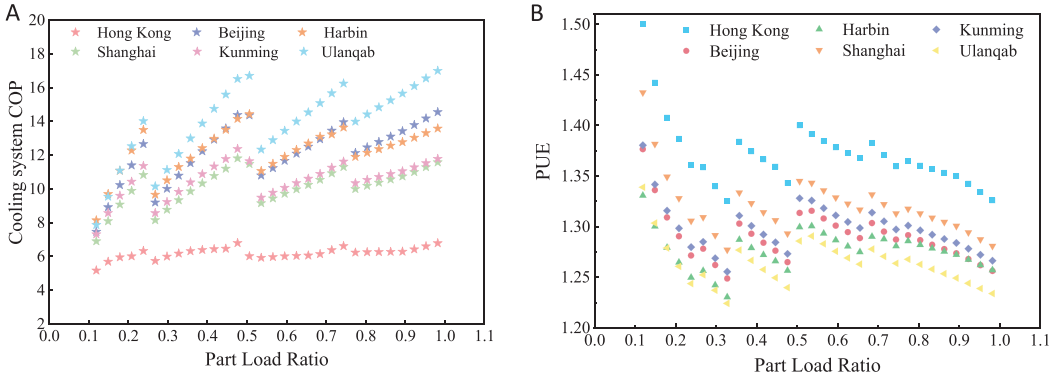


Fig. 11 Annual average cooling system COP (A) and data center PUE (B) under full-range cooling loads in different cities

conditions for free cooling, with the highest number of hours below the critical wet-bulb temperature.

Harbin is characterized as an extremely cold region with harsh winter weather conditions. Consequently, closed-circuit cooling towers are adopted in Harbin, along with the use of an antifreeze solution to prevent freezing. Ulanqab benefits from a more favorable climate with consistently cool temperatures throughout the year. In Ulanqab, only electric heaters are required to address freezing concerns. It is worth noting that the cooling efficiency of closed-circuit cooling towers is lower than that of open cooling towers because the cooling water is not in direct contact with the outdoor cold air (Taylor 2012). Furthermore, antifreeze solutions have a lower thermal conductivity than water, leading to a certain decrease in the cooling system's efficiency in Harbin.

Figure 11(B) compares data center PUE in six cities at different PLRs. Among these cities, Ulanqab exhibits the lowest PUE due to its excellent climate conditions and higher cooling efficiency. In addition, it can be observed that there are some slight fluctuations in PUE, except for the three major fluctuations in PUE due to the switch of chiller numbers. These slight fluctuations are attributed to changes in the number of computer room air handlers in operation at different PLRs.

3.3 Life-cycle energy performance under progressive loading

The IT load within data centers is not static but experiences a progressive increase throughout their lifecycle, as shown in Figure 12(A) (Rasmussen 2011). The expected load of the data center starts at 30% and gradually ramps up to a final expected load value of 90%. However, it is worth noting that the actual start-up load is around 20% of the design load, gradually increasing to an ultimate actual load of approximately 60% of the design capacity. This indicates that most data centers operate at part load for the majority of their lifetime (Griffin 2015). The final achieved IT load is significantly lower than the initial design IT load. This progressive loading characteristic poses challenges to the high-efficiency operation of the cooling system throughout the data center's lifespan. As the IT load increases gradually, the cooling system may not operate at its optimal efficiency, leading to higher energy consumption and potential inefficiencies in cooling capacity utilization.

Figure 12(B) illustrates the difference between the design cooling system COP and the actual cooling system COP in Beijing. It is observed that there is a significant gap between the design COP and the actual COP. The average cooling system COP throughout the lifecycle with the progressive increase in IT load is only 11.7, 2.9 lower than the design system COP. This indicates that the multi-chiller cooling system operates inefficiently for a major portion of its operational lifetime, resulting in substantial energy waste. In addition, it is noticeable that there is also a relatively low cooling system COP throughout the lifespan of the data center under the expected IT load increase. Figure 13 shows the energy performance of the cooling system under an assumption of a 20-year life cycle (also adopting the progressive loading profile from reference (Rasmussen 2011). It is observed that the cooling system operates at a system COP of 11.7 for the majority of its lifetime. However, it is important to note that further analysis of the energy performance of the cooling system is needed if the progressive loading profile differs.

The primary reason behind the inefficiency is that during the design phase, designers typically focus on the design IT load and incorporate extra capacity for emergencies. However, they often overlook the progressive increase in IT load and the ultimate IT load that the data center will experience. As a result, the cooling system is often oversized and the match between the capacity and the quantity of cooling system components is not optimal, which would adversely affect the overall efficiency of the cooling system over the data center's lifetime.

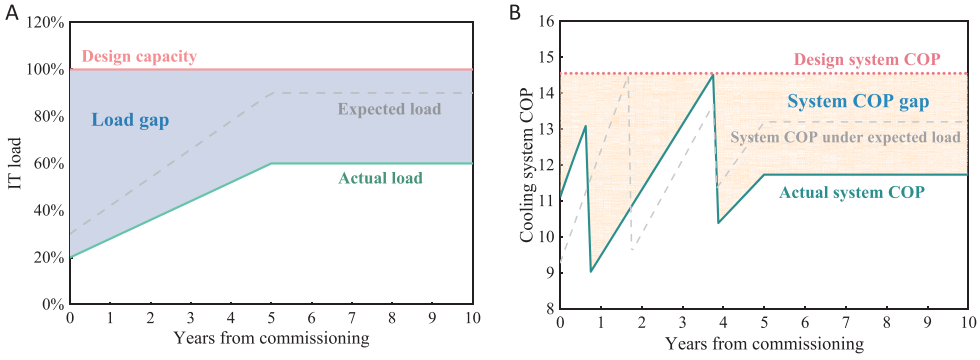


Fig. 12 A typical IT load growth (A) and cooling system COP (B) over a lifetime of 10 years

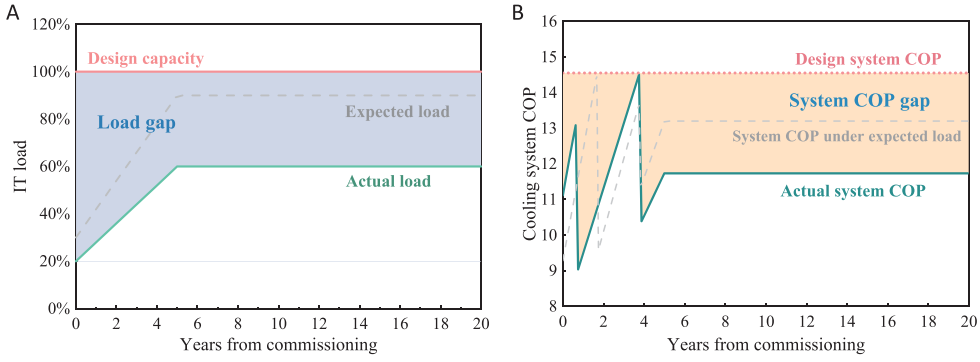


Fig. 13 A typical IT load growth (A) and cooling system COP (B) over a lifetime of 20 years

To address this issue, it is crucial to consider the progressive loading nature of data centers when designing and operating the cooling system. This includes optimizing the cooling system design to match the evolving IT load profile, implementing adaptive control strategies to adjust cooling capacity in response to changing demands, and utilizing load modulation techniques to optimize energy efficiency during part load conditions. By considering these factors, data center operators and designers can mitigate the energy inefficiencies associated with progressive loading and achieve greater energy efficiency throughout the data center's lifetime.

4 Discussion

The energy efficiency of data center cooling systems varies significantly at different part load ratios. The current prevailing designs are largely inefficient in overall lifecycle operation, resulting in significant energy waste. To address this inefficiency, it is imperative for the future design and operation of data centers to take into account the progressive nature of IT load increases. This involves the optimization of the cooling system design to match the evolving IT load profile and the implementation of adaptive control strategies to adjust cooling capacity in response to changing demands. By considering these factors, data center operators and designers can mitigate the energy inefficiencies associated with progressive loading and achieve greater energy efficiency throughout the data center's lifetime.

This study focuses on a typical progressive load profile to assess the energy performance of data center cooling systems. However, in practical scenarios, different data centers will exhibit varying progressive load profiles. Therefore, it is essential to conduct a comprehensive energy performance assessment to design optimal systems tailored to specific progressive load profiles.

5 Conclusions

This study presents a pioneering assessment and quantification of the energy performance of multi-chiller cooling systems in data centers concerning progressive loading throughout the lifecycle. Through an extensive analysis of the energy performance of cooling system components under full-range cooling loads and wet-bulb temperatures, the significant impacts of progressive loading on cooling system COP, data center PUE, and free cooling hours are identified. The key findings and their implications are presented as follows.

The wet-bulb temperatures ranging from 3°C to 9°C play a crucial role in determining the switch of operation modes at different part load ratios (PLRs). The sudden

increases in power consumption observed in the cooling system components primarily occur at PLRs of 0.25, 0.5, and 0.75, due to the increase in cooling equipment quantity in operation.

The performance of the cooling system in different climate conditions is primarily determined by the annual distribution of wet-bulb temperatures. Extreme cold regions require special design considerations for freeze protection, which may result in a decrease in cooling efficiency.

There is a notable variance in cooling system COP at different PLRs. The difference in cooling system COP at different PLRs can be as high as 6, corresponding to a difference in PUE up to 0.14. Additionally, free cooling time could differ up to 1442 hours at different PLRs in the same location. Furthermore, on average, the cooling system COP throughout the lifecycle with a progressively increasing IT load is 2.9 lower than the COP under design conditions.

This study offers critical insights into the energy performance of multi-chiller cooling systems in air-cooled data centers and presents quantified results that can inform the development of next-generation, high-efficiency cooling solutions. By addressing the challenges identified and adopting the recommended strategies, the data center industry can move towards more sustainable and energy-efficient operations. The quantitative results offer valuable insights for designing optimal cooling systems and achieving high-efficiency HVAC systems and cooling plants for data centers, particularly at partial loads throughout the lifecycle.

Acknowledgements

The research of this paper is financially supported by a collaborative research fund (C5018-20G) and a grant under the Hong Kong PhD Fellowship Scheme of the Research Grants Council in the Hong Kong SAR.

Funding note: Open access funding provided by The Hong Kong Polytechnic University.

Declaration of competing interest

The authors have no competing interests to declare that are relevant to the content of this article. Shengwei Wang is an Editorial Board member of *Building Simulation*.

Author contribution statement

Yingbo Zhang: software, formal analysis, investigation, writing—original draft; Hangxin Li: formal analysis, methodology; Shengwei Wang: conceptualization, methodology, supervision, writing—review & editing, funding acquisition.

Open Access: This article is licensed under a Creative Commons Attribution 4.0 International License, which permits use, sharing, adaptation, distribution and reproduction in any medium or format, as long as you give appropriate credit to the original author(s) and the source, provide a link to the Creative Commons license, and indicate if changes were made.

The images or other third party material in this article are included in the article's Creative Commons license, unless indicated otherwise in a credit line to the material. If material is not included in the article's Creative Commons license and your intended use is not permitted by statutory regulation or exceeds the permitted use, you will need to obtain permission directly from the copyright holder.

To view a copy of this license, visit http://creativecommons.org/licenses/by/4.0/

References

ASHRAE (2009). Best Practices for Datacom Facility Energy Efficiency, 2nd edn. Atlanta, GA, USA: American Society of Heating, Refrigerating and Air-Conditioning Engineers.

ASHRAE (2020). ASHRAE Handbook HVAC Systems and Equipment. Atlanta, GA, USA: American Society of Heating, Refrigerating and Air-Conditioning Engineers.

ASHRAE (2021). Thermal Guidelines for Data Processing Environments, 5th edn. Alanta, GA, USA: American Society of Heating, Refrigerating and Air-Conditioning Engineers.

Brady GA, Kapur N, Summers JL, et al. (2013). A case study and critical assessment in calculating power usage effectiveness for a data centre. *Energy Conversion and Management*, 76: 155–161.

Braun JE (1988). Methodologies for the design and control of central cooling plants. PhD Thesis, The University of Wisconsin-Madison, USA.

Capozzoli A, Primiceri G (2015). Cooling systems in data centers: state of art and emerging technologies. *Energy Procedia*, 83: 484–493.

Chen X, Tu R, Li M, et al. (2023). Hot spot temperature prediction and operating parameter estimation of racks in data center using machine learning algorithms based on simulation data. *Building Simulation*, 16: 2159–2176.

Cheung H, Wang S (2019). Optimal design of data center cooling systems concerning multi-chiller system configuration and component selection for energy-efficient operation and maximized free-cooling. *Renewable Energy*, 143: 1717–1731.

Cho J, Yang J, Lee C, et al. (2015). Development of an energy evaluation and design tool for dedicated cooling systems of data centers: Sensing data center cooling energy efficiency. *Energy and Buildings*, 96: 357–372.

Díaz AJ, Cáceres R, Torres R, et al. (2020). Effect of climate conditions on the thermodynamic performance of a data center cooling system under water-side economization. *Energy and Buildings*, 208: 109634.

Gözcü O, Özada B, Carfi MU, et al. (2017). Worldwide energy analysis of major free cooling methods for data centers. In: Proceedings of 2017 16th IEEE Intersociety Conference on Thermal and Thermomechanical Phenomena in Electronic Systems (ITherm), Orlando, FL, USA.

Gözcü O, Erden HS (2019). Energy and economic assessment of major free cooling retrofits for data centers in Turkey. *Turkish Journal of Electrical Engineering & Computer Sciences*, 27: 2197–2212.

Griffin B (2015). Data center economizer efficiency. *ASHRAE Journal*, 57(3): 64–70.

Green Grid (2007). Describing datacenter power efficiency. Green Grid Technical Committee White Paper.

Gupta R, Asgari S, Moazamigoodarzi H, et al. (2020). Cooling architecture selection for air-cooled Data Centers by minimizing exergy destruction. *Energy*, 201: 117625.

Habibi Khalaj A, Halgamuge SK (2017). A Review on efficient thermal management of air- and liquid-cooled data centers: From chip to the cooling system. *Applied Energy*, 205: 1165–1188.

Ham S-W, Kim M-H, Choi B-N, et al. (2015a). Energy saving potential of various air-side economizers in a modular data center. *Applied Energy*, 138: 258–275.

Ham SW, Kim MH, Choi BN, et al. (2015b). Simplified server model to simulate data center cooling energy consumption. *Energy and Buildings*, 86: 328–339.

Iyengar M, Schmidt R, Caricari J (2010). Reducing energy usage in data centers through control of Room Air Conditioning units. In: Proceedings of 2010 12th IEEE Intersociety Conference on Thermal and Thermomechanical Phenomena in Electronic Systems, Las Vegas, NV, USA.

Joshi Y, Kumar P (2012). Energy Efficient Thermal Management of Data Centers. New York: Springer Science & Business Media.

Lei N, Masanet E (2020). Statistical analysis for predicting location-specific data center PUE and its improvement potential. *Energy*, 201: 117556.

Li J, Li Z (2020). Model-based optimization of free cooling switchover temperature and cooling tower approach temperature for data center cooling system with water-side economizer. *Energy and Buildings*, 227: 110407.

Liu Y, Yang X, Li J, et al. (2018). Energy savings of hybrid dew-point evaporative cooler and micro-channel separated heat pipe cooling systems for computer data centers. *Energy*, 163: 629–640.

Liu P, Kandasamy R, Ho JY, et al. (2023). Dynamic performance analysis and thermal modelling of a novel two-phase spray cooled rack system for data center cooling. *Energy*, 269: 126835.

Lu Y, Wang S, Zhao Y, et al. (2015). Renewable energy system optimization of low/zero energy buildings using single-objective and multi-objective optimization methods. *Energy and Buildings*, 89: 61–75.

Lyu W, Wang Z, Li X, et al. (2022). Energy efficiency and economic analysis of utilizing magnetic bearing chillers for the cooling of data centers. *Journal of Building Engineering*, 48: 103920.

Ma Z, Wang S, Xu X, et al. (2008). A supervisory control strategy for building cooling water systems for practical and real time applications. *Energy Conversion and Management*, 49: 2324–2336.

Ma K, Liu M, Zhang J (2020). An improved particle swarm optimization algorithm for the optimization and group control of water-side free cooling using cooling towers. *Building and Environment*, 182: 107167.

Malone C, Belady C (2006). Metrics to characterize data center & IT equipment energy use. In: Proceedings of the Digital Power Forum, Richardson, TX, USA.

Masanet E, Shehabi A, Lei N, et al. (2020). Recalibrating global data center energy-use estimates. *Science*, 367: 984–986.

Mi R, Bai X, Xu X, et al. (2023). Energy performance evaluation in a data center with water-side free cooling. *Energy and Buildings*, 295: 113278.

Mitchell-Jackson J, Koomey JG, Nordman B, et al. (2003). Data center power requirements: measurements from Silicon Valley. *Energy*, 28: 837–850.

Niemann J, Bean J, Avelar V (2011). Economizer modes of data center cooling systems. Schneider Electric Data Center Science Center Whitepaper, 160.

Rasmussen N (2011). Avoiding costs from oversizing data center and network room infrastructure. Schneider Electric Data Center Science Center Whitepaper, 37.

Stabat P, Marchio D (2004). Simplified model for indirect-contact evaporative cooling-tower behaviour. *Applied Energy*, 78: 433–451.

Taylor ST (2012). Optimizing design & control of chilled water plants: Part 4: Chiller & cooling tower selection. *ASHRAE Journal*, 54(3): 60–70.

Taylor ST (2014). How to design & control waterside economizers. *ASHRAE Journal*, 56(6): 30–36.

Wang S (2009). Intelligent Buildings and Building Automation. London: Routledge.

Zhang Y, Li H, Wang S (2023). The global energy impact of raising the space temperature for high-temperature data centers. *Cell Reports Physical Science*, 4: 101624.

Zhou W, Sun Q, Luo W, et al. (2023). Performance analysis and optimization of free cooling strategies for a liquid-cooled data center. *Building Simulation*, 16: 1317–1330.

Zou S, Zhang Q, Yue C (2023). Comparative study on different energy-saving plans using water-side economizer to retrofit the computer room air conditioning system. *Journal of Building Engineering*, 69: 106278.